Article

Investigation of CO_2 solubility in monoethanolamine hydrochloride based deep eutectic solvents and physical properties measurements

Khatereh Ali Pishro, Ghulam Murshid *, Farouq Sabri Mjalli, Jamil Naser

Department of Petroleum & Chemical Engineering, Sultan Qaboos University, Muscat, Oman

ABSTRACT

Deep eutectic solvents (DESs) have drawn a growing research interest for applications in a wide range of scientific and industrial arenas. However, a limited effort has been reported in the area of gas separation processes and particularly the carbon dioxide capture. This study introduces a novel set of DESs that were prepared by complexing ethylenediamine (EDA), monoethanolamine (MEA), tetraethylenepentamine (TEPA), triethylenetetramine (TETA) and diethylenetriamine (DETA) as hydrogen bond donors to monoethanolamide hydrochloride (EAHC) salt as a hydrogen bond acceptor. The absorption capacity of CO_2 was evaluated by exploiting a method based on measuring the pressure drop during the absorption process. The solubility of different DESs was studied at a temperature of 313.15 K and initial pressure of 0.8 MPa. The DES systems 1EAHC:9DETA, 1EAHC:9TETA and 1EAHC:9TEPA achieved the highest CO_2 solubility of 0.6611, 0.6572 and 0.7017 mol $CO_2 \cdot (\text{mole DES})^{-1}$ respectively. The results showed that CO_2 solubility in the DESs increased with increasing the molar ratio of hydrogen bond donor. In addition, the CO_2 solubility increased as the number of amine groups in the solvent increases, therefore, increasing the alkyl chain length in the DESs, resulted in increasing the CO_2 solubility. FTIR analysis confirms the DES synthesis since no new functional group was identified. The FTIR spectra also revealed the carbamate formation in DES-CO_2 mixtures. In addition, the densities and viscosities of the synthesized DESs were also measured. The CO_2 initial investigation of reported DESs shows that these can be potential alternative for conventional solvents in CO_2 capture processes.

© 2020 The Chemical Industry and Engineering Society of China, and Chemical Industry Press. All rights reserved.

1. Introduction

Over the past decades, increasing concern about the global warming encouraged the scientific community to focus on CO_2 capture as CO_2 is considered a major cause of the greenhouse phenomenon. In 2013, CO_2 levels surpassed 400 ppm for the first time in recorded history [1,2], and the reduction of CO_2 released to the atmosphere became a major focus of research. Consequently, particular attention was directed towards the latest developments in CO_2 separation techniques, which removes CO_2 using cost-effective technologies. For more thorough discussions on solvents used for CO_2 separation, the reader may refer to a number of excellent in-depth reviews in the field [3–5].

The most established and industrially approved CO_2 capture technology is to use aqueous amine absorbents. Amine-based technologies are well thought out as leading other alternatives. Nevertheless, these technologies have serious drawbacks such as solvent degradation, [6] equipment corrosion, energy intensive solvent regeneration and high operational costs [7]. Therefore, while developments in amine-based solvents were proposed to solve the aforementioned problems, the

development of new solvents for CO_2 capture with better characteristics has attracted great attention [8].

Ionic liquids (ILs) offer a new opportunity and are a very promising alternative absorbent option for improving the post-combustion CO_2 capture [9,10] Wide interest in ILs arises from a general need for new green and environmental friendly solvents to replace conventional ones, which present several problems such as inherent toxicity or high volatility [11]. Many of the physicochemical properties of ILs are very suitable for CO_2 capture, such as low flammability, negligible vapor pressure, and high thermal stability [11, 12]. Nevertheless, in spite of all these possible benefits, the literature has also reported some practical limitations of these ILs such as toxicity, low biodegradability, and unfavorable high production cost [13].

Deep eutectic solvents (DESs) are emerging as successful alternatives to ILs with similar features and benefits. A DES is a mixture of two or more components with a melting point lower than its individual components. DESs are typically obtained by mixing a quaternary ammonium or phosphonium salt, as a hydrogen-bond acceptor (HBA), with one or more components that are capable of donating hydrogen bonds (hydrogen bond donor (HBD) molecule). The HBD-HBA complexation leads to a significant depression in the freezing point of the mixture. DESs have noticeable advantages over ILs such as simple

synthesis, lower cost, and biodegradable nature for some cases. Since the first choline chloride-urea DES reported by Abbott *et al.* [14] other combinations of HBDs and HBAs have been reported and used for many successful applications. A wide range of chemical and industrial applications of DESs were investigated in the past few decades. Some of these applications include biochemical, electrochemical, catalysis, chemical synthesis and most importantly material separation [15].

Several studies have reported the application of ionic liquids and DESs as solvents for CO_2 capture [16–21]. The CO_2 loading of these DESs compared with conventional Ionic liquids capture was reported [22–26]. As a matter of fact, the CO_2 solubility data is limited to only few reported DESs and therefore more work is needed to develop novel gas absorbents. In a recent study, Trivedi *et al.* [27] introduced a new class of DESs that exhibited relatively high CO_2 uptakes by employing ethylenediamine (EDA) as a HBD and monoethanolamide hydrochloride which prepared by adding hydrogen chloride (HCl) to monoethanolamine (MEA) as an HBA, the highest CO_2 loading value among all the existing DES was achieved. The similar studies suggested that DESs can be regarded as strong candidates to replace conventional monoethanolamine-based scrubbing technology solvents.

The CO_2 solubility of aqueous solutions of five linear polyamines was investigated [28] at 313.15 K and 393.15 K and CO_2 partial pressure of about 1–500 kPa and revealed that CO_2 capture performance is strongly dependent on the chemical species (number of amino groups), the carbon number between the amino groups and the chain length. This study concluded that while Tetraethylenepentamine (TEPA), Triethylenetetramine (TETA), Diethylenetriamine (DETA) are similar in structure, the solubility increases with increasing the number of amino groups and revealed that DETA has the highest absorption capacity based on mole $CO_2 \cdot (kg\ amine)^{-1}$.

Although different types of conventional DESs have been studied, there is still little reported on CO_2 absorption study by amine based DESs [20,28].

This work investigates the absorption capacity of CO_2 by exploiting a measurement method based on determining the pressure drop during the absorption process at a temperature of 313.15 K which is usually a temperature range of operating an industrial absorber [2,29]. The DESs were prepared by adding one of six different HBDs namely; ethylenediamine (EDA), monoethanolamine (MEA), tetraethylenepentamine (TEPA), triethylenetetramine (TETA),

diethylenetriamine (DETA) to monoethanolamide hydrochloride (EAHC) salt as a HBA. Densities and Viscosities were also measured for the prepared DESs as these properties are important in designing the absorber and in mass transfer calculations as well. The FTIR analysis was also conducted for the studied DES to analyze the interaction mechanism between CO_2 and DESs and probable reaction mechanism is also established.

2. Experimental

2.1. Chemicals used

The Ethanolamine hydrochloride (EAHC) was purchased from Sigma-Aldrich. All HBDs including ethylenediamine (EDA), monoethanolamine (MEA), tetraethylenepentamine (TEPA), triethylenetetramine (TETA) and diethylenetriamine (DETA) were supplied by Sigma-Aldrich.

Solubility is strongly dependent on the chemical specification such as; number of amino groups, configuration of the chemical structure, and the carbon number between the amino groups and the chain length. EDA, MEA and EAHC; salt of MEA have shown a short and simple structure of amine solvents. Besides, TEPA, TETA, and DETA are similar in structure, but the chain length is longer in TEPA than the other two chemicals in order.

These chemicals were used without any further purification. Fig. 1 shows the molecular structure of all chemicals and Table 1 lists the specification of chemicals and gases used in this study. Purified food grade Carbon dioxide (CO_2) gas with purity of 99.99% and nitrogen (N_2) gas with purity of 98% were used in this work. Both gases were purchased from a local gas supplier.

2.2. Preparation of DESs mixtures

The method of DESs preparation is explained in previous studies [14,30,31]. The DESs were prepared with the same EAHC to HBDs ratios of 1:1, 1:3, 1:6 and 1:9. EAHC was mixed with HBDs using a magnetic stirrer equipped with a temperature control assembly. The mass of all pure components were measured with a digital balance (Shimadzu, model AUW220D), with an estimated accuracy of ± 0.1 mg. Each combination of EAHC and the selected HBD was mixed at 400 r·min^{-1} for at least 3 h at atmospheric pressure and temperature between 343.15 K
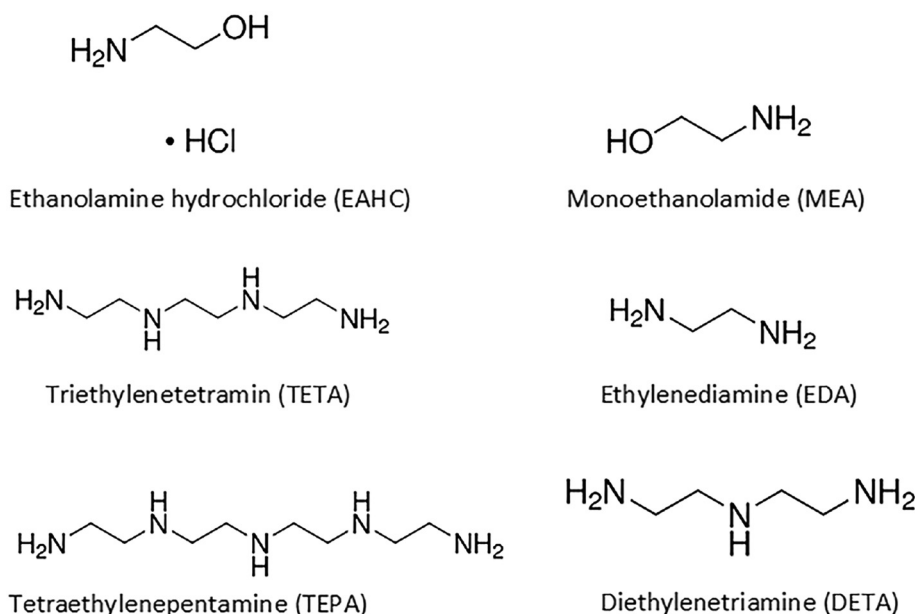

Fig. 1. Chemical structures of salt and HBDs.

Table 1
List of chemicals and gases used in this work

Chemicals and gases	CAS no.	Supplier	Molecular weight/g·mol^{-1}	Purity
EAHC	2002-24-6	Sigma-Aldrich	97.54	0.99
MEA	141-43-5	Sigma-Aldrich	61.08	0.99
DETA	111-40-0	Sigma-Aldrich	103.16	0.95
EDA	107-15-3	Sigma-Aldrich	60.1	0.897
TETA	112-24-3	Sigma-Aldrich	146.23	0.98
TEPA	112-57-2	Sigma-Aldrich	189.3	0.998
Carbon dioxide (CO_2)	–	Muscat Int. gas	44.01	0.999
Nitrogen (N_2)	–	Muscat Int. gas	28.014	0.98

and 353.15 K in a fume hood. The stirring was continued until a homogeneous liquid without any precipitation was formed. These are then stored in tight sealed bottles kept in vacuum fume hood. Table 2 shows the abbreviations, molar ratio of salt and HBDs and appearance at room temperature of prepared DESs.

In some cases, a yellowish color was noticed as shown in Fig. 2 Since the stability of DESs is very important, the prepared DES samples were kept in the lab for at least two days and monitored for any phase separation. The chemical structure of the DESs was investigated using FTIR analysis. In order to prevent moisture and any contamination, all chemicals were isolated in a humidity controlled condition.

2.3. CO$_2$ solubility measurement

The pressure drop method is one of the widely reported techniques for CO$_2$ solubility measurement [29,32,33]. The volume of solvent is kept constant and the pressure drop is recorded. It is well known that

Table 2
Abbreviations, molar ratio of salt and HBDs in liquid and the appearance of liquid at room temperature of prepared DESs

DESs molar ratios	DESs abbreviations	Appearance of the liquids
1EAHC:1MEA	DES 1	Transparent yellow
1EAHC:3MEA	DES 2	Transparent yellow
1EAHC:6MEA	DES 3	Transparent yellow
1EAHC:9MEA	DES 4	Transparent yellow
1EAHC:1DETA	DES 5	Transparent colorless
1EAHC:3DETA	DES 6	Transparent colorless
1EAHC:6DETA	DES 7	Transparent colorless
1EAHC:9DETA	DES 8	Transparent colorless
1EAHC:1EDA	DES 9	Transparent colorless
1EAHC:3EDA	DES 10	Transparent colorless
1EAHC:6EDA	DES 11	Transparent colorless
1EAHC:9EDA	DES 12	Transparent colorless
1EAHC:1TETA	DES 13	Transparent yellow
1EAHC:3TETA	DES 14	Transparent yellow
1EAHC:6TETA	DES 15	Transparent yellow
1EAHC:9TETA	DES 16	Transparent yellow
1EAHC:1TEPA	DES 17	Transparent yellow
1EAHC:3TEPA	DES 18	Transparent yellow
1EAHC:6TEPA	DES 19	Transparent yellow
1EAHC:9TEPA	DES 20	Transparent yellow

solvents such as DESs have negligible vapor pressure; hence, an assumption was made that the gaseous phase remains Pure [34]. The pressure drop method is simple, precise, and requires less computational effort to determine accurate gas absorption. Consequently, in this study, the pressure drop method was used to measure CO$_2$ solubility. All measured properties are reported with standard uncertainties.

The solubility measurements were made in a medium-pressure solubility cell as shown in the Fig. 3. The experimental setup used in this work is similar to the one used by Haris *et al.* It consists of two vessels; pressure vessel (150 ml) where the gas pressure is maintained at a desired level to transfer to the equilibrium vessel (50 ml). The equilibrium cell is where the solubility measurements were made based on the pressure drop method. The whole setup was immersed in a water bath to achieve the desired temperature. Initially, both cells were purged with nitrogen and then CO$_2$ was transferred directly from the cylinder to the pressure vessel and a desired pressure (0.8 MPa) was maintained, with a pressure gage (Crystal control, METEK, nvision), estimated accuracy of ± 0.001 MPa. Vacuum pump was used to remove the contaminations in the equilibrium cell and 6 ml of DES solution was introduced into the cell using metering pump. The measurements were similar to the work reported by Jenab *et al.* and Park *et al.* [33]. The temperature of the cell was then adjusted to the desired value using Julabo circulator heater with measuring accuracy of ± 0.03 K. The CO$_2$ was transferred from pressure vessel to the equilibrium cell and the stirrer was turned on. The moles of CO$_2$ transferred from the pressure vessel were calculated by the following Eq. (1) [29] .

$$n_{CO_2} = \frac{V_T}{RT_a}\left(\frac{P_1}{Z_1} - \frac{P_2}{Z_2}\right) \tag{1}$$

Where V_T is the volume of the gas container (pressure vessel), Z_1 and Z_2 are the compressibility factors for each pressure (P_1 and P_2) are calculated from Peng-Robinson equation of state [35], R is the gas constant and T_a is the ambient temperature. The equilibrium was achieved in 7 h to 9 h. The equilibrium pressure (P_{CO2}) was recorded and the moles of CO$_2$ in a gas phase were calculated by the following Eq. (2).

$$n_{CO_2}^g = \frac{V_g P_{CO_2}}{Z_{CO_2} RT} \tag{2}$$

Where V_g is the gas volume in the equilibrium cell and T is the operating temperature. The moles of CO$_2$ in the liquid phase were then calculated from

$$n_{CO_2}^l = n_{CO_2} - n_{CO_2}^g \tag{3}$$

The solubility was then calculated as mol of CO$_2$ per mol of the solvent mixture by using the following Eq. (4). The experimental uncertainty of measured CO$_2$ solubility values at corresponding temperature was estimated to be as ± 3 × 10^{-3} mol·mol^{-1} and ± 0.03 K, respectively.

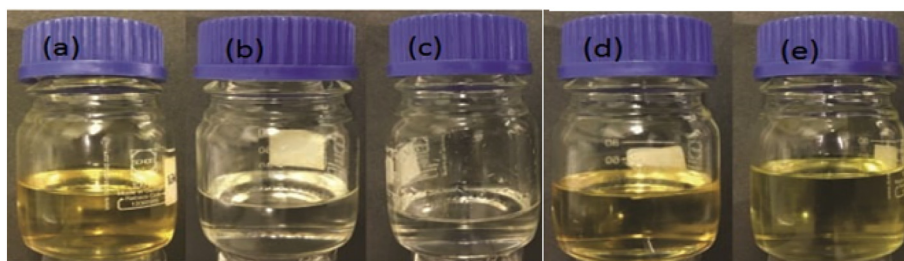$$\alpha = \frac{n_{CO_2}^l}{n_{solvent}} \tag{4}$$

Fig. 2. Appearance of prepared DESs: (a). EAHC-MEA; (b). EAHC-DETA; (c). EAHC-EDA; (d). EAHC-TETA; (e). EAHC-TEPA.
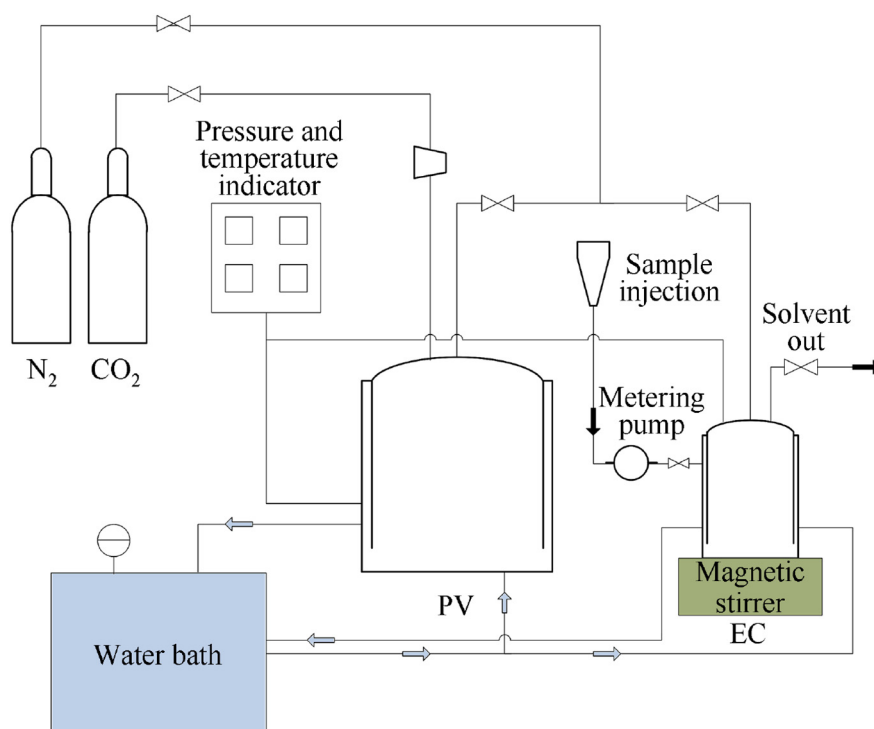
Fig. 3. Schematic diagram of solubility equipment; PV: Pressure Vessel and EC: Equilibrium Cell.

2.4. Density measurement

Density of prepared samples was measured using Anton Paar DMA-4500M vibrating tube density meter with measuring accuracy of $\pm 1.0 \times 10^{-4}$ g·cm^{-3}. The sample was injected in to the tube using an injection syringe, this method of measuring density was reported by Mjalli, *et al.* [36]. The density meter was calibrated before each measurement with water of Millipore quality. All of the densities were measured at a temperature range of (303.15 to 333.15) K with a temperature controlled accuracy of ± 0.01 K (PT 100). The experimental uncertainty of measured density at corresponding temperature was estimated to be as $\pm 3 \times 10^{-4}$ g·cm^{-3} and ± 0.01 K, respectively. The desired temperature was set and the tube is subjected to vibrations until the resonance frequency is reached. This frequency is directly proportional to the density of the sample. The reported density is an average of three measurements.

2.5. Viscosity measurement

Kinematic viscosities of non-aqueous system of different DESs at 40 °C were measured using a calibrated Ubbelohde Viscometer (Cannon-Fenske) of appropriate size. The samples were immersed in a thermostatic bath (Tamson, TVB445) for at least 15 min with temperature controlled accuracy of 0.02 K. this method for viscosity measurement is also reported elsewhere [8]. The efflux time was then measured using a stopwatch with an accuracy of 0.01 s. The viscosity values were reproducible within $\pm 1\%$ with reported temperature uncertainty of ± 0.02 K. The dynamic viscosities were calculated by multiplying the corresponding density with kinematic viscosities.

2.6. FTIR measurement

Some finalized DESs shown in Table 2 were found to have a yellowish color, accordingly, these ratios were analyzed using FTIR to investigate possible chemical reactions among the DES species during the preparation stage. The Infrared spectra of the DESs were obtained in the range of 4000–650 cm^{-1} on a Perkin-Elmer Spectrum 400 ATR-IR instrument.

3. Results and Discussion

In order to ensure the reliability and accuracy of the reported data, the density and viscosity of known pure components reported in literature were measured and compared. This comparison was performed using an average absolute deviation (AAD) as given below and reported in Table 3.

$$\text{AAD} = \left(\frac{1}{N}\right) \sum_{i=1}^{N} \mid \frac{Y_i^{\text{exp}} - Y_i^{\text{lit}}}{Y_i^{\text{exp}}} \mid \times 100\% \qquad (5)$$

where N is the number of experimental data points. The subscripts "exp" and "lit" represent the experimental and literature value of a quantity respectively. The lower computed values of AADs given in Table 3 suggest the reliability and accuracy of the equipment used to investigate the thermophysical property data [37]. However, a slight variation observed between the experimental and literature values can be attributed to the variations in procedures, equipment accuracies, and purities of the utilized chemicals.

Table 3
Experimental and literature reported density and viscosity data of 20 mass % AHPD and the corresponding average absolute deviation [37]

Temperature/K	ρ/g·m^{-3}			η/mPa·s		
	Expt.	Lit.	AAD/%	Expt.	Lit.	AAD/%
303.15	1.0475	1.0474	0.0120	1.472	1.475	0.130
313.15	1.0432	1.0434		1.169	1.170	
323.15	1.0391	1.0390		0.963	0.962	
333.15	1.0331	1.0330		0.783	0.782	

Similarly, the solubility equipment was also calibrated. To calibrate the experimental apparatus and verify the accuracy of the measurement, the solubility of CO_2 in aqueous 30 wt% Monoethanolamine (MEA) solution at 313.15 K. Table 4 shows the CO_2 solubility measurement results along with their standard deviations. The results indicate a good agreement between the data obtained in this work, and the reported in literature [38].

Table 4
Comparison of measured CO_2 solubility in 30 wt% of MEA solution at 313.15 K with available data in literature

P_{CO2}/MPa	α CO_2 (this study)	α CO_2 (lit [38])	AAD/%
0.552	0.665	0.676	2.215
0.883	0.709	0.728	
1.256	0.748	0.763	
1.580	0.753	0.772	

Density and viscosity of all twenty synthesized DESs data is presented in Table 5 and also presented in Figs. 4 and 5 at temperature of

Table 5
Density and viscosity of synthesized DESs at 40 °C

No.	DESs	Viscosity η/mPa·s	Density/g·cm^{-3}
DES 1	1EAHC:1MEA	0.112	1.1503
DES 2	1EAHC:3MEA	0.048	1.0898
DES 3	1EAHC:6MEA	0.029	1.0559
DES 4	1EAHC:9MEA	0.021	1.0424
DES 5	1EAHC:1DETA	0.390	1.0990
DES 6	1EAHC:3DETA	0.052	1.0272
DES 7	1EAHC:6DETA	0.014	0.9863
DES 8	1EAHC:9DETA	0.009	0.9751
DES 9	1EAHC:1EDA	0.113	1.0302
DES 10	1EAHC:3EDA	0.042	1.0218
DES 11	1EAHC:6EDA	0.009	0.9696
DES 12	1EAHC:9EDA	0.004	0.9435
DES 13	1EAHC:1TETA	0.728	1.0974
DES 14	1EAHC:3TETA	0.134	1.0639
DES 15	1EAHC:6TETA	0.052	1.0315
DES 16	1EAHC:9TETA	0.036	0.9981
DES 17	1EAHC:1TEPA	2.398	1.1151
DES 18	1EAHC:3TEPA	0.257	1.0281
DES 19	1EAHC:6TEPA	0.103	1.0081
DES 20	1EAHC:9TEPA	0.070	0.9971

40 °C respectively. Density data shows that the density decreases by increasing the ratio of HBD in all synthesized DESs irrespective of the type of HBD. Similar trend was reported in ChCl-MEA based DES. This shows that by adding the HBD the volume of the solution increases. This could also be due to increase in the repulsion forces between HBD and the salt [39,40]. However, the decrease in the density in all DESs is not significant. The DEA 1 measured the highest density which is 1.1504 g·cm^{-3} and the lowest is DES 12 which is 0.9435 g·cm^{-3}, respectively. This shows that all synthesized DESs behave in a similar way in terms of molecular interactions. The hole theory [39,40] can also be applied to explain the densities of DESs that density depends upon the packing or the molecular structure of the DES.

The viscosity data of all synthesized DESs is presented in Fig. 5 at the same temperature of 40 °C. The viscosity of all DESs decreases by increasing the amount of HBD in the DES mixture. This shows that the addition of amines to the mixture helps to reducing its resistance to flow. The similar phenomenon is noticed in the CO_2 solubility results as well, which are presented in next section. Higher solubility was achieved in DES with low viscosities. This could be due to better mixing and mass transfer between gas and liquid at low viscosities.

The DES 17 was reported with the highest dynamic viscosity *i.e.* 2.3986 Pa·s and the lowest was that attained by DES 12. It can be observed that the viscosity tends to decrease with the increase in the HBD amount in the mixture and this decrease can be seen in all synthesized DES irrespective of the HBD structure.

As can be seen from the viscosity data, the DES containing smaller HBD molecules attain lower viscosity compared to those with larger molecular structure. The order of these HBD ranked from highest to lowest is TEPA (DES17-20)>TETA (DES13-16)>DETA (DES5-8)>EDA (DES9-12)>MEA (DES1-4). In addition, increasing the HBD content in the DES results in a noticeable reduction in viscosity. This is more pronounced in the case of large molecular sized HBD like TEPA. This can be explained in terms of the hole theory which attributes the increase of viscosity of solvents having large radii to the probability of encountering voids of suitable sizes for then to move into [14,40].

3.1. FTIR analysis of prepared DESs

The FTIR spectra of synthesized DESs with molar composition of 1:9 are also represented in Fig. 6. The FTIR results confirm the formation of DES as from the reported spectra, all the functional groups of both constituents were identified. The FTIR peaks of reported DESs broadened as compare to pure amines at ~2800 cm^{-1}. The broadening of O—H stretching of EAHC at 3500 cm^{-1} and 2500 cm^{-1}, indicates the formation of hydrogen bonds between EAHC and HBDs in DES.
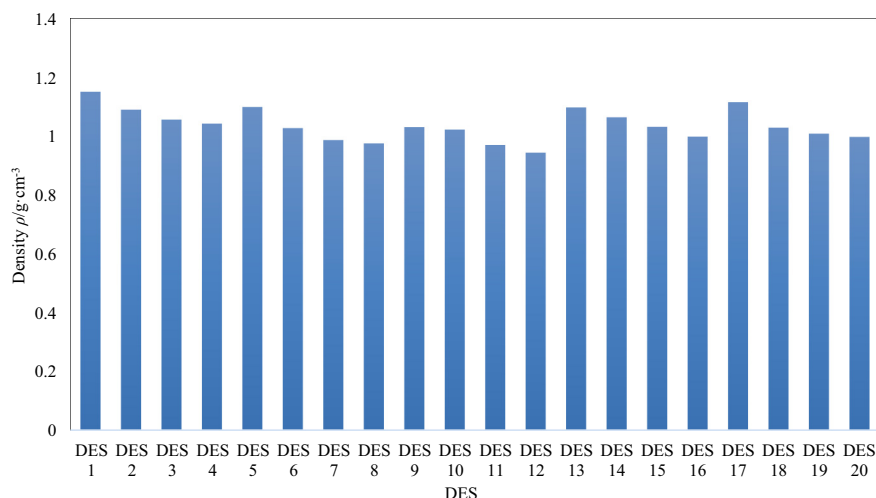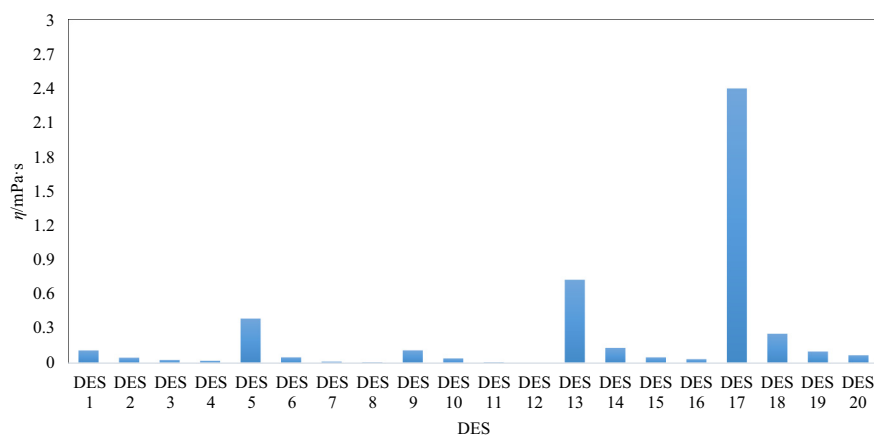

Fig. 4. Density of synthesized DESs at 40 °C.

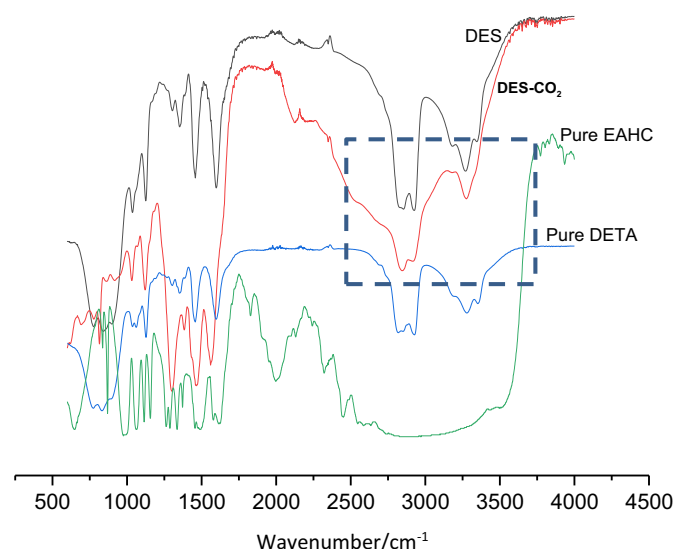**Fig. 5.** Viscosity of synthesized DESs at 40 °C.

Fig. 6. FT-IR spectra of EAHC:DETA (1:9), before and after CO$_2$ absorption, pure DETA and pure EAHC.

3.2. Suggested reaction mechanism

The reaction mechanism of the chemisorption involved between the studied solvents and carbon dioxide is depicted in Fig. 7. The binding of CO$_2$ with [EAHC][DETA] can be explained by the formation of carbamic acid upon reaction with CO$_2$. The carbamate was then formed due to de-protonation of COOH as COO$^-$ and protonation of amine as NH$_4^+$ forming the carbamate [EAHC][DETA][CO$_2$].

As shown in The FTIR spectra of DES-CO$_2$ (1EAHC:9DETA) in Fig. 6, the peak of primary amine at 2925 cm^{-1} is slightly diminished as compared to the sharp peaks of primary amine at 2825 cm^{-1} and 2925 cm^{-1} in DES which shows the presence of carbamate formation. This is further supported by the broadening of peaks from 3400 to 2800 cm^{-1} due to formation of hydrogen boding as compared to the peaks in the same region in FTIR of DETA. Appearance of peak at ~1600 cm^{-1} in the DES-CO$_2$ further confirmed the formation of carbamate [41].

3.3. Solubility of CO$_2$ in DESs

3.3.1. Effect of HBD and molar ratio on CO$_2$ Solubility

The prepared DESs were used without any further purification to study the CO$_2$ intake at 0.8 MPa and 313.15 K. The intake is reported as (α), mole CO$_2 \cdot$ (mole DES)$^{-1}$. The loading capacity data of all prepared DESs is presented in Table 6. The solubility of CO$_2$ in solutions
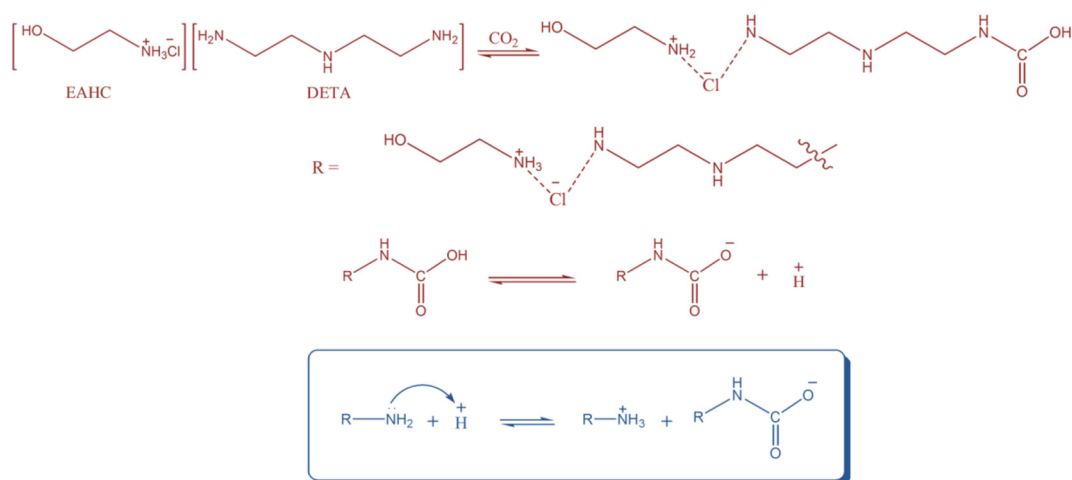

Fig. 7. The suggested structure for the formation of DES intermolecular network based on the interaction between ammonium and the established carbamate.

Table 6
CO_2 solubility in prepared DESs at 313.15 K and 0.8 MPa

No.	DESs	p/MPa	$\alpha\ CO_2$
DES 1	1EAHC:1MEA	0.830	0.164
DES 2	1EAHC:3MEA	0.833	0.173
DES 3	1EAHC:6MEA	0.822	0.224
DES 4	1EAHC:9MEA	0.811	0.274
DES 5	1EAHC:1DETA	0.842	0.258
DES 6	1EAHC:3DETA	0.845	0.406
DES 7	1EAHC:6DETA	0.829	0.561
DES 8	1EAHC:9DETA	0.855	0.661
DES 9	1EAHC:1EDA	0.834	0.201
DES 10	1EAHC:3EDA	0.843	0.289
DES 11	1EAHC:6EDA	0.834	0.485
DES 12	1EAHC:9EDA	0.858	0.501
DES 13	1EAHC:1TETA	0.811	0.272
DES 14	1EAHC:3TETA	0.837	0.504
DES 15	1EAHC:6TETA	0.829	0.562
DES 16	1EAHC:9TETA	0.851	0.657
DES 17	1EAHC:1TEPA	0.851	0.272
DES 18	1EAHC:3TEPA	0.852	0.382
DES 19	1EAHC:6TEPA	0.822	0.594
DES 20	1EAHC:9TEPA	0.846	0.702
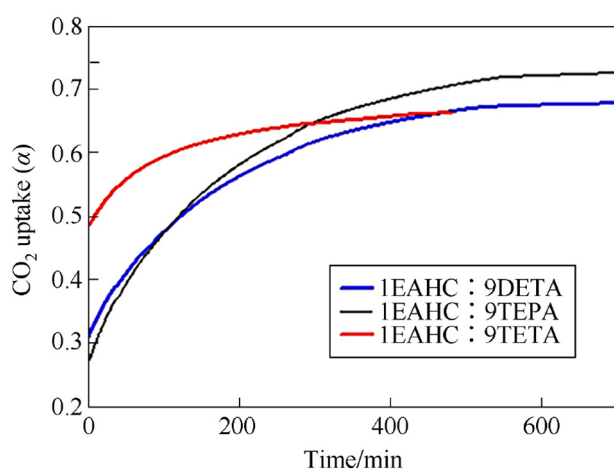
depends on several factors such as the strength of hydrogen bond within the DESs structure, molar ratio, molecular weight of DES and alkyl chain length [30]. It was reported that as the alkyl chain length in ILs and DESs increased, the solubility increased [28,42], which is in agreement with the reported data in this work for various DESs in Table 6. The highest CO_2 uptake is observed for the DESs; 1EAHC:9DETA, 1EAHC:9TETA and 1EAHC:9TEPA as shown in the Table 6. The uptake for the above three DESs at 0.8 MPa and 313.15 K is 0.6611, 0.6572 and 0.7017 $mol \cdot mol^{-1}$ respectively. It is observed that the CO_2 solubility increases as the number of amine groups in the chemical structure from DETA, TETA and TEPA of the solvent molecule increases. Therefore, increasing the alkyl chain length in the studied DESs, leads to CO_2 solubility increase as shown in Table 6. Similar trends for the CO_2 loading (α) were reported [43,44].

The increase of CO_2 uptake for each DES system as the molar ratio of the HBD increases could be attributed to the drop in the DES viscosity as shown in Fig. 5. This leads to increasing the fluidity of the solvent and consequently improving mass transfer.

3.3.2. The Dynamic study of CO_2 capture

Fig. 8 represents the dynamics of CO_2 capture for the best three studied DESs. The three solvents achieved comparable final CO_2 uptake. However, it is evident that the DES 1EAHC:9TETA attained the fastest response as it achieves its equilibrium uptake within around 300 min while the other two needed another 200 min. Fast CO_2 uptake dynamics is very important for minimizing the gas-solvent needed contact time and consequently higher process throughput. In general, the long time for reaching equilibrium indicates that using such systems needs long retention times and consequently large reactor volume which is a limitation that needs to be further investigated.

3.3.3. The solubility data in comparison with literatures

The data was also compared with reported literature for deep eutectic solvents as shown in Fig. 9. Comparison of CO_2 solubility of the prepared DES (1EAHC:9TEPA) with the reported data involving the salts of choline chloride (ChCl) [45], *n*-butyltriphenylphosphonium bromide (BTPPBr), methyltriphenylphosphonium bromide (MTPPBr), tetrabutylammonium bromide (TBABr) [20] and monoethanolamine hydrochloride (EAHC), triethanolamine chloride (TEAC), thioacetamide chloride (TAEC), ethylenediamine chloride (EDAC), [27] as well as the industrial standard 30 wt% MEA [38], at the same temperature 313.15

Fig. 8. Evolution of CO_2 uptake (α) as a function of time for the best three DESs studied.
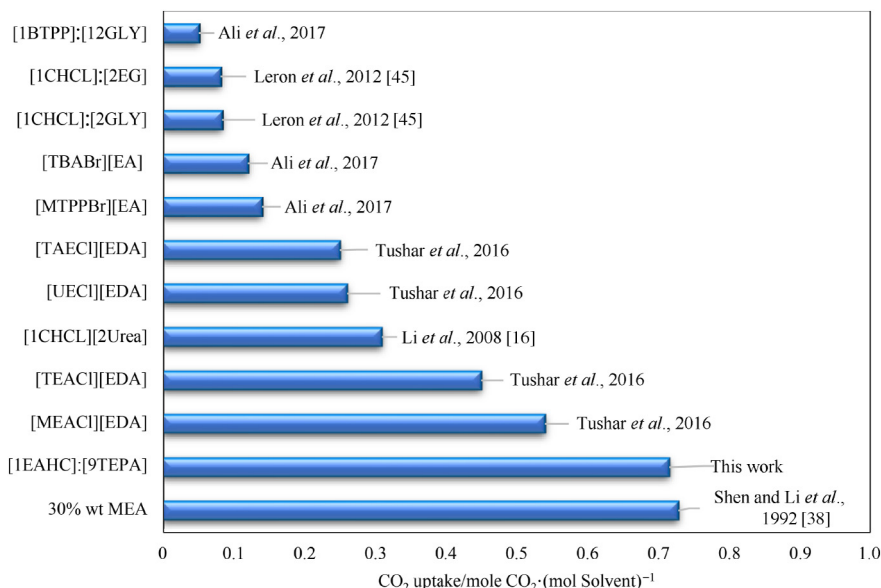
Fig. 9. Comparison of CO_2 solubility of prepared DEtS, 1EAHC:9TEPA with reported data at the same temperature 313.15 K.

K and different pressure shows a significant improvement of the studied DESs to be used for CO_2 absorption as potential replacement of conventional aqueous amines solutions.

4. Conclusions

The solubility of CO_2 in a novel monoethanolamine hydrochloride-based DES and any of ethylene diamine (EDA), monoethanolamine (MEA), tetraethylenepentamine (TEPA), triethylenetetramine (TETA), diethylenetriamine (DETA) as HBDs was investigated in this work. The HBA-HBD combinations of these compounds show homogeneous stable mixtures at molar ratios of 1:1, 1:3, 1:6 and 1:9. The FTIR analysis confirmed the DES synthesis since no new functional groups were identified. The spectra of DES-CO_2 indicate the carbamate formation. The densities and viscosities were also measured and reported.

The absorption of CO_2 was measured at a temperature of 313.15 K and pressure of around 0.8 MPa. Among the studies systems, the three systems: 1EAHC:9DETA, 1EAHC:9TETA and 1EAHC:9TEPA exhibited the highest CO_2 solubility. These new solvents show competing performance to the conventional amine-based industrial solvent. In addition to the well-known merits of these eutectic solvents including their low preparation cost, the eco-friendly nature, low vapor pressure and chemical structure tunability, the newly presented solvents exhibited high CO_2 absorption capacity which suggests presenting them as promising alternatives to the tradition monoethanolamine-based solvents.

Acknowledgements

References

[1] T.H. Oh, Carbon capture and storage potential in a coal-fired plant in Malaysia - A review, Renew. Sust. Energ. Rev. 14 (9) (2010) 2697–2709.
[2] S. Inoue, T. Itakura, T. Nakagaki, Y. Furukawa, S. Hiroshi, Y. Yasuro, Experimental study on CO_2 solubility in aqueous piperazine/alkanolamines solutions at stripper conditions, Energy Procedia 37 (2013) 1751–1759.
[3] A.D. Ebner, A.R. James, State-of-the-art adsorption and membrane separation processes for carbon dioxide production from carbon dioxide emitting industries, Sep. Sci. Technol. 44 (6) (2009) 1273–1421.
[4] S. Choi, J.H. Drese, W.J. Christopher, Adsorbent materials for carbon dioxide capture from large anthropogenic point sources, ChemSusChem 2 (9) (2009) 796–854.
[5] M.P. Suh, Y.E. Cheon, E.Y. Lee, Syntheses and functions of porous metallosupramolecular networks, Cood. Chem. Rev. 252 (8–9) (2008) 1007–1026.
[6] L. Raynal, P.A. Bouillon, A. Gomez, P. Broutin, From MEA to demixing solvents and future steps, a roadmap for lowering the cost of post-combustion carbon capture, Chem. Eng. J. 171 (3) (2011) 742–752.
[7] S. Garg, G. Murshid, F.S. Mjalli, W. Ahmad, Physical properties of aqueous blend of diethanolamine and sarcosine: experimental and correlation study, Chem. Pap. 71 (10) (2017) 1799–1807.
[8] G. Murshid, H. Ghaedi, M. Ayoub, W. Ahmad, Experimental and correlation of viscosity and refractive index of non-aqueous system of diethanolamine (DEA) and dimethylformamide (DMF) for CO_2 capture, J. Mol. Liq. 250 (2018) 162–170.
[9] D.R. MacFarlane, N. Tachikawa, M. Forsyth, J.M. Pringle, P.C. Howlett, G.D. Elliott, C.A. Angell, Energy applications of ionic liquids, Energy Environ. Sci. 7 (1) (2014) 232–250.
[10] F.A. Chowdhury, H. Okabe, H. Yamada, M. Onoda, Y. Fujioka, Synthesis and selection of hindered new amine absorbents for CO_2 capture, Energy Procedia 4 (2011) 201–208.
[11] B. Peric, J. Sierra, E. Martí, R. Cruañas, M.A. Garau, J. Arning, S. Stolte, (Eco) toxicity and biodegradability of selected protic and aprotic ionic liquids, J. Hazard. Mater. 261 (2013) 99–105.
[12] M. Smiglak, W.M. Reichert, J.D. Holbrey, J.S. Wilkes, L. Sun, J.S. Thrasher, R.D. Rogers, Combustible ionic liquids by design: is laboratory safety another ionic liquid myth? ChemComm (24) (2006) 2554–2556.
[13] A.P. Abbott, G. Capper, D.L. Davies, R.K. Rasheed, V. Tambyrajah, Novel solvent properties of choline chloride/urea mixtures, ChemComm 1 (2003) 70–71.
[14] E.L. Smith, A.P. Abbott, K.S. Ryder, Deep eutectic solvents (DESs) and their applications, Chem. Rev. 114 (21) (2014) 11060–11082.
[16] X. Li, M. Hou, B. Han, X. Wang, L. Zou, Solubility of CO_2 in a choline chloride + urea eutectic mixture, J. Chem. Eng. Data 53 (2) (2008) 548–550.
[17] R.B. Leron, A. Caparanga, M.H. Li, Carbon dioxide solubility in a deep eutectic solvent based on choline chloride and urea at T = 303.15–343.15 K and moderate pressures, J. Taiwan Inst. Chem. Eng. 44 (6) (2013) 879–885.
[18] M. Francisco, A. Bruinhorst, L.F. Zubeir, C.J. Peters, M.C. Kroon, A new low transition temperature mixture (LTTM) formed by choline chloride + lactic acid: Characterization as solvent for CO_2 capture, Fluid Phase Equilib. 340 (2013) 77–84.
[19] L.L. Sze, S. Pandey, S. Ravula, S. Pandey, H. Zhao, G.A. Baker, S.N. Baker, Ternary deep eutectic solvents tasked for carbon dioxide capture, ACS Sustain. Chem. Eng. 2 (9) (2014) 2117–2123.
[20] E. Ali, M.K. Hadj-Kali, S. Mulyono, Solubility of CO_2 in deep eutectic solvents: experiments and modelling using the Peng–Robinson equation of state, Chem. Eng. Res. Des. 92 (10) (2014) 1898–1906.
[21] B.E. Gurkan, J.C. de la Fuente, E.M. Mindrup, Equimolar CO_2 absorption by anion-functionalized ionic liquids, J. Am. Chem. Soc. 132 (7) (2010) 2116–2117.
[22] Y. Zhang, S. Zhang, X. Lu, Q. Zhou, W. Fan, X. Zhang, Dual amino-functionalised phosphonium ionic liquids for CO_2 capture, Chem. Eur. J. 15 (12) (2009) 3003–3011.
[23] S. Saravanamurugan, A.J. Kunov-Kruse, R. Fehrmann, A. Riisager, Amine-functionalized amino acid-based ionic liquids as efficient and high-capacity absorbents for CO_2, Chem Sus Chem 7 (3) (2014) 897–902.
[24] C. Wang, X. Luo, H. Luo, D.E. Jiang, H. Li, S. Dai, Tuning the basicity of ionic liquids for equimolar CO_2 capture, Angew. Chem. 123 (21) (2011) 5020–5024.
[25] X. Luo, Y. Guo, F. Ding, Significant improvements in CO_2 capture by pyridine-containing anion-functionalized ionic liquids through multiple-site cooperative interactions, Angew. Chem. 126 (27) (2014) 7173–7177.
[26] J. Zhang, C. Jia, H. Dong, J. Wang, X. Zhang, S. Zhang, A novel dual amino-functionalized cation-tethered ionic liquid for CO_2 capture, Ind. Eng. Chem. Res. 52 (17) (2013) 5835–5841.
[27] T.J. Trivedi, J.H. Lee, H.J. Lee, H.J. Lee, Y.K. Jeong, J.W. Choi, Deep eutectic solvents as attractive media for CO_2 capture, Green Chem. 18 (9) (2016) 2834–2842.
[28] W.M. Budzianowski, Energy Efficient Solvents for CO_2 Capture by Gas-liquid Absorption, Springer, 2017.
[29] M.K. Park, O.C. Sandall, Solubility of carbon dioxide and nitrous oxide in 50 mass methyldiethanolamine, J. Chem. Eng. Data 46 (1) (2001) 166–168.
[30] H. Ghaedi, M. Ayoub, S. Sufian, CO_2 capture with the help of Phosphonium-based deep eutectic solvents, J. Mol. Liq. 243 (2017) 564–571.
[31] B. Jibril, F. Mjalli, J. Naser, New tetrapropylammonium bromide-based deep eutectic solvents: synthesis and characterizations, J. Mol. Liq. 199 (2014) 462–469.
[32] F. Harris, K.A. Kurnia, M.I.A. Mutalib, Solubilities of carbon dioxide and densities of aqueous sodium glycinate solutions before and after CO_2 absorption, J. Chem. Eng. Data 54 (1) (2009) 144–147.
[33] M.H. Jenab, M.A. Abdi, S.H. Najibi, Solubility of carbon dioxide in aqueous mixtures of N-methyldiethanolamine plus piperazine plus sulfolane, J. Chem. Eng. Data 50 (2) (2005) 583–586.
[34] K. Shahbaz, F.S. Mjalli, G. Vakili-Nezhaad, Thermogravimetric measurement of deep eutectic solvents vapor pressure, J. Mol. Liq. 222 (2016) 61–66.
[35] B.K. Mondal, S.S. Bandyopadhyay, A.N. Samanta, VLE of CO_2 in aqueous sodium glycinate solution–new data and modeling using Kent–Eisenberg model, Int. J. Greenh. Gas Con. 36 (2015) 153–160.
[36] F.S. Mjalli, G. Murshid, S. Al-Zakwani, A. Hayyan, Monoethanolamine-based deep eutectic solvents, their synthesis and characterization, Fluid Phase Equilib. 448 (2017) 30–40.
[37] J. Park, S.J. Yoon, H. Lee, J.H. Yoon, J.G. Shim, J.K. Lee, H.M. Eum, Density, viscosity, and solubility of CO_2 in aqueous solutions of 2-Amino-2-hydroxymethyl-1, 3-propanediol, J. Chem. Eng. Data 47 (4) (2002) 970–973.
[38] K.P. Shen, M.H. Li, Solubility of carbon dioxide in aqueous mixtures of monoethanolamine with methyldiethanolamine, J. Chem. Eng. Data 37 (1) (1992) 96–100.
[39] M.H. Shafie, R. Yusof, C.Y. Gan, Synthesis of citric acid monohydrate-choline chloride based deep eutectic solvents (DES) and characterization of their physicochemical properties, J. Mol. Liq. 288 (2019), 111081. .
[40] A.P. Abbott, G. Capper, S. Gray, Design of improved deep eutectic solvents using hole theory, ChemPhysChem 7 (4) (2006) 803–806.
[41] G. Murshid, F.S. Mjalli, J. Naser, S. Al-Zakwani, A. Hayyan, Novel diethanolamine based deep eutectic mixtures for carbon dioxide (CO_2) capture: Synthesis and characterisation, Phys. Chem. Liq. (2018) 473–490.
[42] R.B. Leron, M.H. Li, Solubility of carbon dioxide in a choline chloride–ethylene glycol based deep eutectic solvent, Thermochim. Acta 551 (2013) 14–19.
[43] P. Singh, G.F. Versteeg, Structure and activity relationships for CO_2 regeneration from aqueous amine-based absorbents, Process Saf. Environ. 86 (5) (2008) 347–359.
[44] H. Machida, H. Yamada, Y. Fujioka, CO_2 solubility measurements and modeling for tertiary diamines, J. Chem. Eng. Data 60 (3) (2015) 814–820.
[45] R.B. Leron, A.N. Soriano, M.H. Li, Densities and refractive indices of the deep eutectic solvents (choline chloride + ethylene glycol or glycerol) and their aqueous mixtures at the temperature ranging from 298.15 to 333.15 K, J. Taiwan Inst. Chem. E. 43 (4) (2012) 551–557.